

# Preparation and Characterisation of Self-Assembled Dye Fibers

Maxime FRUH

*Carlos Rodriguez-Abreu, Institute for Advanced Chemistry of Catalonia, Spanish National Research Council (IQAC-CSIC) and Networking Research Center on Bioengineering, Biomaterials and Nanomedicine(CIBER-BBN), Barcelona, Spain*

**Abstract**— Two types of fibers have been prepared by self-assembly. The first system is made of Astrophloxine hydrogel fibers, based on the stacking of molecules by  $\pi$ - $\pi$  interactions. Various properties of the hydrogel have been characterized with UV-vis absorbance, Fluorescence spectroscopy, calorimetric profiles, and rheology. The hydrogel shows temperature-dependent fluorescence. Above the melting temperature  $T > 44^\circ\text{C}$ , fluorescence and hydrogel structure are lost, but they are recovered upon cooling, demonstrating that the process is reversible. The fibers also showed a temperature-dependent birefringency. The second system of fibers was formed by ionic self-assembly (ISA) of two oppositely charged dyes. This system was characterized by SEM and TEM, as well as X-Ray diffraction. The ISA fibers were able to encapsulate a drug, showing promise for controlled drug release.

**Index Terms**— Institute IQAC-CSIC. Dye self-assembled fibers, fluorescent fibers, hydrogel,  $\pi$ - $\pi$  stacking, ionic interaction, drug encapsulation.

## I. INTRODUCTION

**N**ANOTECHNOLOGY is a field based on the size-dependent properties of materials, that has allowed the development of new systems that are more efficient, smarter and with new properties. One of the fields in which nanotechnology is having an impact is medicine [1]. There are limitations for many drugs to be successful, from the low water solubility, insufficient targeting and delivery. The new types of formulations developed nowadays thanks to nanotechnologies are able to out pass those limitations, making the systems more effective, less toxic, with less or without side effects, and with a possible drug delivery control.

Several methods exist for the synthesis of nanomaterials. Self assembly is a bottom-up strategy for the fabrication of nanomaterials that consists in a spontaneous arrangement of nanoscale building blocks into a stable and well-ordered structure through non-covalent interactions like hydrogen bonds, van der Waals forces, hydrophobic and electrostatic interactions. The development of systems using self-assembly is interesting as it is a simple and fast way to synthesize nanoscale building blocks[2]. Especially, ionic self-assembly (ISA), described first in 2003 by Faul [3], which is based on electrostatic interactions, presents advantages such as reliability, flexibility and cost savings, which is particularly

interesting as it can easily be scalable for high production. At the same time it is possible to create very complex systems with adjustable properties.

Dye molecules are known to self-assemble in solution, and are ideal as contain diverse functional groups with a specific structure, known as extended  $\pi$  systems [4]–[6]. In some dyes such as cyanines, aromatic and double bonds are connected allowing the  $\pi$  electrons to travel freely all over the surface of the molecule. Due to the fact that the molecular structure is flat, all the molecules can easily stack on each other and self-assemble thanks to the  $\pi$ - $\pi$  interactions. It is this stacking that leads to the formation of long, fiber-like aggregates.

Cyanine dyes, which excitation/emission in the near-infrared (NIR), are very interesting for biomedical applications such as biological probes, *e.g.* drug delivery, as their fluorescent properties fit into the “imaging window” in which the light absorption of biological material is minimum[7].

Herein, two types of self-assembled fibers were developed. The first type is induced by  $\pi$ - $\pi$  interactions between the molecules, which form a hydrogel. The second type of fibers is formed by ISA of two oppositely charged molecules. The properties and structure of both types of fibers were characterized and their potential for drug encapsulation was explored in preliminary experiments.

### *Objective:*

Throughout this paper, the synthesis, the characterisation and the drug encapsulation process will be explained for each system.

The objective, in the case of the hydrogel system, was to characterize the different optical properties -such as the excitation/emission profile, fluorescence profile- and viscoelastic properties to highlight the temperature dependent behaviour.

The objective in the second system was the optimization of a protocol for the synthesis of fibers with small size -high surface to volume ratio- and high drug encapsulation capacity, followed by the characterization of optical, crystalline and drug encapsulation properties.

## II. EXPERIMENTS

### A. Materials

Astrophloxine Iodate manufactured by TCI with a purity of 98%, Quinaldine Red Iodate manufactured by Sigma-Aldrich with a purity of 95% and Sunset Yellow manufactured by Sigma-Aldrich with a purity of 90% were used in the experiments as self-assembling dyes. The structures of these dyes are shown in *Figure 1* and *Figure 2*.

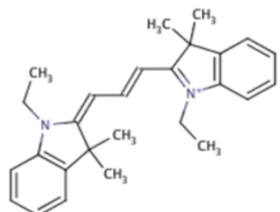


**Figure 1-** Molecular structure of Astrophloxine used in the preparation of hydrogel fibers.

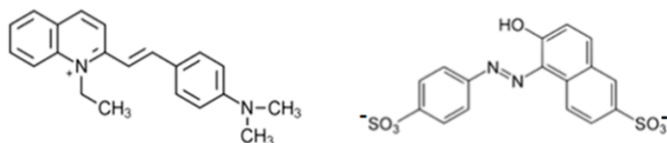


**Figure 2-** Molecular structure of Quinaldine Red on the left and of Sunset yellow on the right, used in the preparation of ISA based fibers.

Silver Acrylate manufactured by ABCR with a purity of 95% and Silver Acetate manufactured by ABCR with a purity of 99% were also used.

The drug used as reference for the drug encapsulation is Ketoprofen, an ibuprofen-type nonsteroidal anti-inflammatory agent with analgesic and antipyretic properties [8], manufactured by Sigma-Aldrich with a purity >98%. See *Figure 3*.

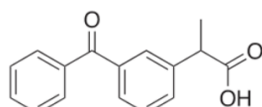


**Figure 3-** Molecular structure of Ketoprofen

### B. Methods

#### **Preparation of Astrophloxine Acrylate:**

Astrophloxine acrylate was used in order to prepare the hydrogel fibers. Since the commercial compound used was the Astrophloxine iodate, it was necessary to change the counter ion from iodate to acrylate. This change was done in order to avoid any salt precipitation or secondary reaction due to the iodate. Astrophloxine was dissolved in methanol ( $[C]=10\text{mmol/L}$ ). Silver acrylate (1:1 equivalent) was added to the Astrophloxine solution and left stirring overnight at room temperature. The day after, the silver iodide precipitate was removed by filtration. The filtrated solution of methanol with the Astrophloxine acrylate was left under nitrogen gas flow in

order to evaporate the methanol, resulting in solid Astrophloxine acrylate.

#### **Preparation of Astrophloxine Acrylate based hydrogel:**

The hydrogel was prepared by dissolution of Astrophloxine acrylate in distilled water. In order to form the hydrogel, two tests of dissolution at different concentration were done. The first one at a concentration of 5%w/v (weight /volume) Astrophloxine and the second one at a concentration of 3%w/v. Distilled water was added to the Astrophloxine acrylate in order to form the hydrogel. For the gel at 5%w/v this step was difficult due to the fact that the gel is highly viscous making the total dissolution of Astrophloxine hard to handle. It was necessary to heat the mixture at 60°C in order to melt the gel and facilitate the dissolution. The dissolution at 3%w/v did not form the hydrogel but remained as a liquid. The second test at 5%w/v resulted in formation of a hydrogel with high viscosity. It is this sample that was used for most of the characterization tests.

#### **Preparation of Quinaldine Red acetate:**

Quinaldine Red (QR) acetate was used for the synthesis of the second system of fibers. Since the commercial compound was the QR iodate, a change of the counter ion was necessary for the same reason described for Astrophloxine acetate.

QR iodate was dissolved in ethanol ( $[C]=125\text{mmol/L}$ ). Silver acetate (1:1 equivalent) was then added to the solution and left stirring all the night at room temperature. The day after, the precipitate of silver iodate was removed by filtration and the ethanol of the filtrated solution was evaporated under nitrogen gas flow in order to obtain the QR acetate as a solid.

#### **Preparation of Quinaldine red acetate-Sunset Yellow fibers by ionic self-assembly and drug encapsulation:**

Fibers were prepared by mixing QR acetate and Sunset Yellow (SY). The drug used as a reference for the encapsulation was the Ketoprofen (KTP). Several types of protocols have been tried for the preparation.

A total dye amount of 50mg was used. QR was added slightly in excess to compensate the presence of KTP (the excess of QR was at 1:1 equivalence with the KTP). In order to have a KTP concentration high enough for the drug release test, 10mg were used in the preparation.

In the first method (Method 1), both dyes, SY and QR, were dissolved separately in 1ml of Phosphate Buffer Saline (PBS). Separately, 10mg of KTP were dissolved in 3mL of PBS. While stirring, 1mL solution of QR was first added to the KTP followed by 1mL solution of SY. The last one was added drop wise. When mixing the QR and SY solution the fibers started to form instantaneously. Then the solution was centrifuged for 5 min at 3000 RPM and the supernatant was removed. A small quantity of the supernatant solution was taken for further HPLC analysis. The fibers were then washed by adding 5mL of distilled water, centrifuged and the supernatant removed 4 times. The fibers were dried left under nitrogen flow.

The second method (Method 2) was based on solvent displacement. KTP and QR were dissolved separately in 1mL of ethanol. Since the SY is not soluble in ethanol, it was dissolved in 5mL PBS solution for the precipitation. KTP and QR solution were mixed together before to be added drop wise to the PBS-SY solution under vortex stirring. Then the solution was centrifuged for 5 min at 3000 RPM and the supernatant was removed. A small quantity of the supernatant solution was taken for further HPLC analysis. The fibers were then washed by adding 5mL of distilled water, centrifuged and the supernatant removed 4 times. The fibers were then dried under nitrogen flow in order to dry them.

#### **Preparation of the PBS solution:**

Due to the low solubility of the Ketoprofen in water, most of the reaction had to be performed in PBS solution where the solubility is much higher [9], [10].

For 1L of PBS at 0.16M, the solution was prepared as followed:

-8g of NaCl

-0.22g of  $\text{NaH}_2\text{PO}_4 \cdot \text{H}_2\text{O}$

-2.98g of  $\text{NaHPO}_4 \cdot 2\text{H}_2\text{O}$

The solution was then adjusted to pH 7.4 with orthophosphoric acid.

#### **High Performance Liquid Chromatography (HPLC):**

HPLC was used to measure the concentrations of KTP for the drug encapsulations tests. A calibration curve as a function of concentration was prepared. The HPLC system consisted of a Water 1525 Binary HPLC Pump, Water 2489 UV/Visible Detector. The condition used for the HPLC were the following: 5min run at 1mL/min flow with 55% flow of B (acetonitrile solution for HPLC) and 45% flow of A (aqueous solution of mQ water at pH=3 with hydrochloric acid). The lamp was at 260nm and the volume of injection was 20 $\mu$ L.

**UV-visible spectrophotometry:** A Cary 300 Bio UV-Visible spectrophotometer was used to determine the absorbance of Astrophloxine. Measurements were done at room temperature using a quartz cuvette of 1cm.

**Fluorescence spectrometry:** An Agilent Cary Eclips instrument was used to measure the fluorescence of Astrophloxine. Path quartz cuvettes of 1cm were used.

**Optical microscopy:** An Olympus BX51TRF-6 microscope was used for the optical characterization of the systems. In order to monitor the evolution of the hydrogel in function of the temperature, a hot stage T95 PE Linkam Scientific instrument Ltd was used.

**Small angle X-Ray scattering (SAXS):** SAXS measurements, done to characterize the 5%w/v Astrophloxine Acrylate hydrogel, were performed using a HECUS X-Ray system GMBH (Graz, Austria) model S3 MICRO, with a  $\text{CuK}\alpha$  anode at 0.1542nm. An MBraun PSD-50 M and 2D detectors were used to record the scattering. Wax-sealed

quartz capillary of 80mm in length, 20mm in diameter and 0.01mm wall thickness were used as support for the sample.

**Rheology:** An AR G2 instrument was used to characterize the viscosity and the viscoelasticity of the Astrophloxine Acrylate hydrogel. The measurements were done using parallel plate of 20mm diameter, a gap of 200micrometer and a temperature of 25°C.

**Scanning Electron Microscopy (SEM):** A TM-1000 Tabletop Microscope from Hitachi was used. The QR-SY ionically self-assembled fibers samples were prepared by depositing fibers dispersion on a glass substrate and evaporating the solvent before measurement. After lyophilisation, the Astrophloxine Acrylate hydrogel samples were deposited directly on a glue surface before measurement.

**Transmission Electron Microscope (TEM):** TEM was performed with a JEOL JEM-2100 microscope at 200kV. Samples were prepared by depositing fibers dispersion on a copper grid covered with a carbon layer. The solvent was then evaporated in order to leave the fibers at the surface of the grid before observation.

**Differential Scanning Calorimeter (DSC):** DSC measurements were done using a micro DCS III Setaram Co instrument. The measurements were done under nitrogen atmosphere, at a speed of 1°C/min.

**X-ray diffraction (XRD):** Powder X-ray diffraction data were collected on a D8 Advance Bruker set at 40 kV and 40 mA, and equipped with a  $\text{Cu K}\alpha$  radiation source ( $\lambda=1.541874 \text{ \AA}$ ).

### III. RESULTS

#### A. Astrophloxine Acrylate fiber-based hydrogels:

##### - Temperature-dependent fluorescence

At room temperature the hydrogel at 5%w/v is highly viscous, however once the temperature is above 50°C, the hydrogel “melt” and becomes liquid. By comparing the fluorescence of the gel at room temperature and at 50°C, we could see that the hydrogel also loses its fluorescence properties once melted. In order to demonstrate the loss of the fluorescence from the hydrogel state to the liquid state, a sample of 5%w/v gel was heated up to around 50°C while another one was left at room temperature (see Figure 4). When leaving the two samples at room temperature under UV light, we could see the fluorescence from the second sample at room temperature, while nothing was seen for the one a 50°C. When cooling down, the first sample was becoming gradually fluorescent until being the same as the second sample at RT.

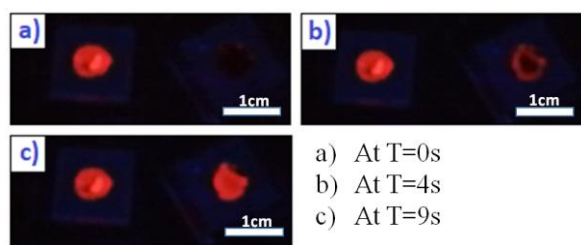


**Figure 4-** Evolution of the fluorescence of Astrophloxine Acrylate hydrogel with temperature, of two samples of the 5%wv hydrogel under UV light. The sample on the left was left at RT all the time while the sample on the right was first at 50°C in the picture a) at time T=0s and then in c) cooled down to room temperature, at time T=9s.

Fluorescence appears to be favoured by the specific interactions between the molecules of Astrophloxine in the solid fibers and which are disrupted upon melting. By heating the molecules, the thermal energy can become higher than the  $\pi$ - $\pi$  interaction energy and the fluorescence disappears [11]. The relation between the fluorescence and the self-assembly of the molecules seems then intrinsic. When the molecules are self-assembled the system is fluorescent and vice versa, when the system is not fluorescent it means that the molecules are not self-assembled anymore in the gel-like state. Thus, it is possible to monitor the reaction of self-assembly using external stimuli: temperature. Since the reaction of self-assembly is spontaneous, by controlling the temperature it is possible to pass from a self-assemble system (presence of the fibers) to a non-self-assembled system (“melting” of the fibers) and vice versa. This process can be monitored by using UV light.

The hydrogel was also observed under optical microscope using a polarizer filter. It was found that Astrophloxine hydrogel is a birefringent system at room temperature. A birefringent system is composed of a molecularly ordered material, where there is double refraction of light due to different refractive indices that are dependent on the orientation of the molecules within the system [12].

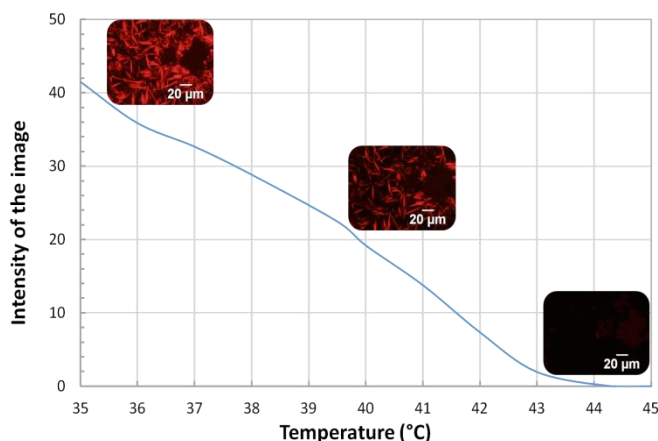


**Figure 5-** Evolution of the birefringence of Astrophloxine Acrylate hydrogel as a function of the temperature. The data treatment from the initial image was done using the software “Imagej” and measuring the intensity of the image. The intensity value given at  $T > 45^\circ\text{C}$  was used as 0.

To obtain the calorimetric profile, the hydrogel was subject to a gradient of temperature and pictures were taken at  $1^\circ\text{C}$  increments. As seen in Figure 5, the intensity of the birefringence decreases as temperature increases, until  $T=44^\circ\text{C}$  where birefringence disappears, and the sample looks black under the polarizers.

Further characterization of the hydrogel was done by Differential Scanning Calorimetry (DSC). In Figure 6, one can clearly see an endothermic peak (with a value of enthalpy J/g: 0.8825) at  $39^\circ\text{C}$  in the heating profile, characteristic to a “melting” process. An exothermic peak (with a value of enthalpy J/g: -0.9021) is also observed in the cooling profile corresponding to a solidification process. The DSC profiles then indicate that the transitions observed in the hydrogel are associated with melting and solidification processes of Astrophloxine aggregates forming the hydrogel.

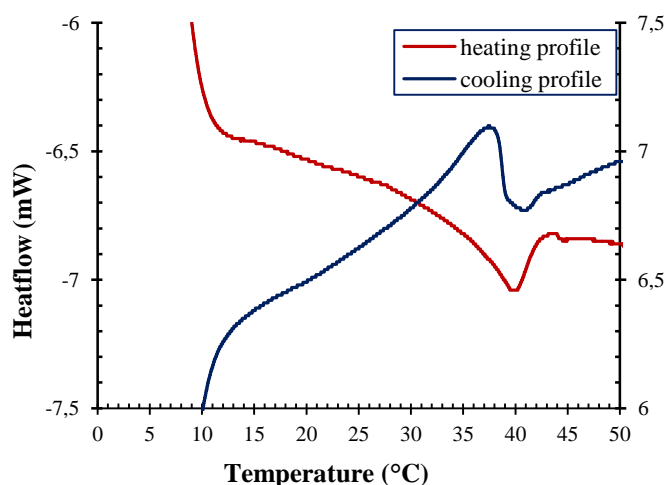


**Figure 6-** Heating and cooling profile of the hydrogel at 5%w/v.

#### - Absorbance/Emission characterization of Astrophloxine Acrylate:

A UV-vis spectrum of Astrophloxine Acrylate was collected. The spectrum in Figure 7 shows a maximum value of absorbance at 540nm.

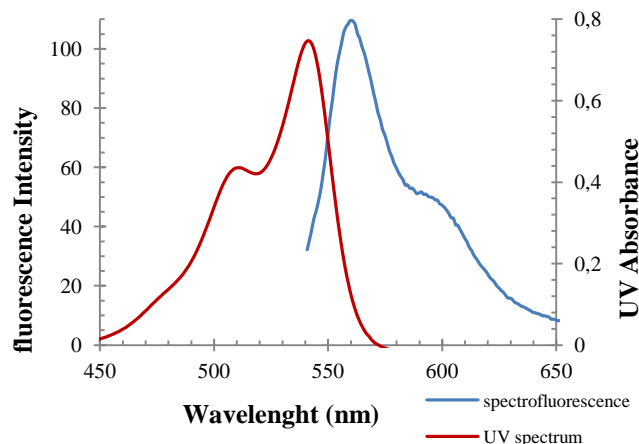


**Figure 7-** Absorption/Emission profiles of Astrophloxine Acrylate in distilled water at room temperature.

The sample was excited at this value of maximum absorbance and a fluorescence emission spectrum was obtained (also in *Figure 7*). Maximum fluorescence intensity was obtained at 560nm.

The structure of the Astrophloxine Acrylate allows  $\pi$ - $\pi$  interaction between the aromatic groups. This leads to a stacking of the molecules and formation of the hydrogel, as shown in *Figure 8*.

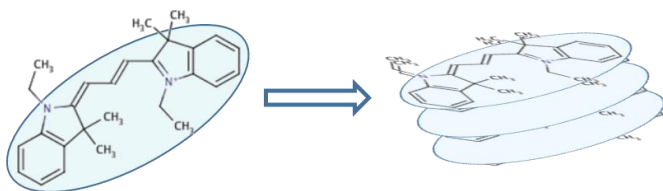


**Figure 8** Scheme of the molecular-arrangement of Astrophloxine Acrylate.

#### - SAXS characterization of Astrophloxine Acrylate hydrogel:

In order to know if the Astrophloxine Acrylate hydrogel showed liquid crystal behaviour, SAXS patterns were collected. As seen in *Figure 9*, no peaks were observed in the SAXS angle range, indicating that there are no liquid crystal-like structures with long range arrangement.

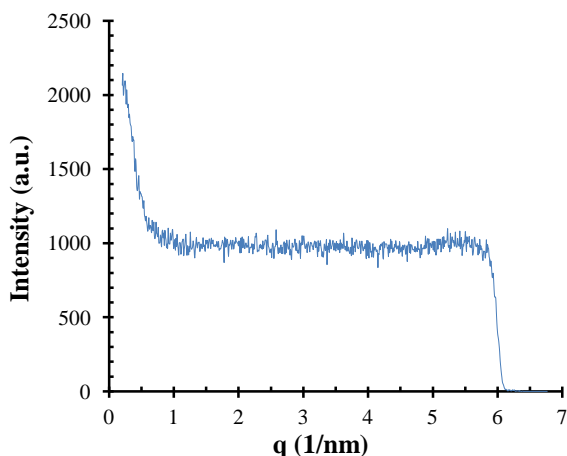


**Figure 9**- SAXS pattern of the 5%w/v hydro gel of Astrophloxine Acrylate.

#### - Rheological characterization of Astrophloxine Acrylate hydrogel:

Rheology test were done to determine the viscosity profile and the viscoelastic properties of the hydrogel (*Figure 10*). The viscosity characterizes the resistance to flow of a material

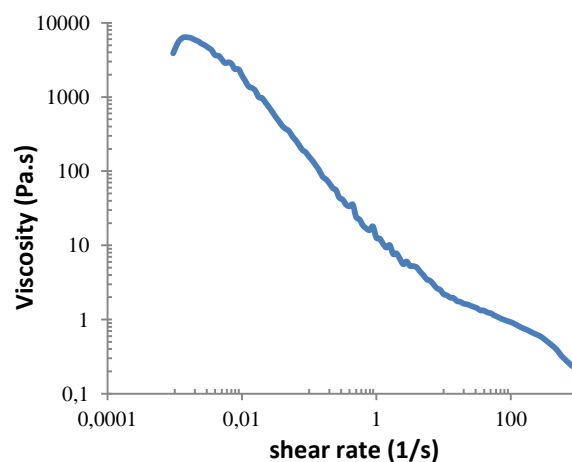


**Figure 10**- Viscosity versus share rate of the 5%w/v Astrophloxine Acrylate hydrogel at 25°C.

As seen in *Figure 10*, viscosity is dependant to the shear rate, therefore the hydrogel behave as a non-Newtonian material, with a shear-thinning typical of a pseudo-plastic material [13]–[15].

The viscoelastic properties of a material are the combination of elastic and viscous behaviour subjected to shear strain[16]. This properties were measured by oscillatory rheometer (see *Figure 11*), in which the material is placed between two parallel plates and an oscillating sinusoidal strain is subjected to the system, while the stress is measured. By applying stress and strain on a material it is possible to determine the storage modulus  $G'$  (elastic parameter) and the loss modulus  $G''$  (viscous parameter). The result from the oscillatory test is plotted as a sine curve with strain versus time, where there is a phase shift  $\delta$  which is the time lag between the present and the resulting oscillation at each point and which values range from  $0^\circ$  to  $90^\circ$ . For a gel-like state,  $\delta$  is between  $0^\circ$ - $45^\circ$ , which means that the material in a normal state is solid [17], [18].

The complex modulus  $G^*$  is obtained from the ratio of the stress amplitude to the strain amplitude. The parameters  $G'$  and  $G''$  can be determined following the formulas:

$$\begin{aligned} G' &= G^* \cos \delta \\ G'' &= G^* \sin \delta \end{aligned}$$

Where  $G'$  gives information about the elastic compartment of a material when is deformed and relates the stress to the strain;  $G''$  reflects how a material flows when is deformed and relates change in strain in time when stopping the applied stress [19].

As expected, the profile is typical of a gel-like material (see *Figure 11*).

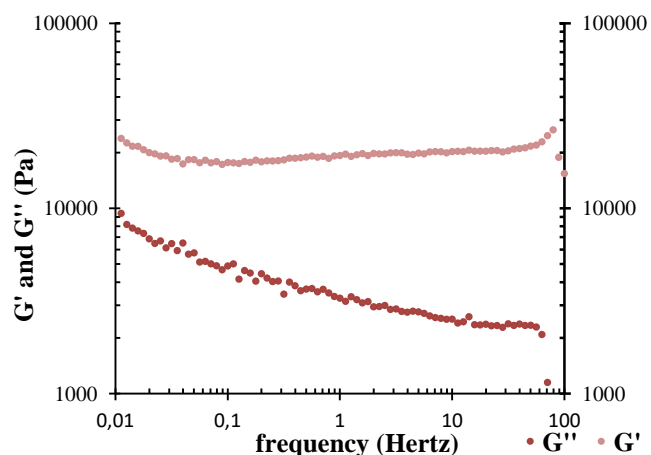


Figure 11 -  $G'$  and  $G''$  versus frequency of oscillation of the 5%w/v.

#### - Characterization of Hydrogel by Microscopy:

By optical microscope the exact structure of the hydrogel could not be determined, but we developed the hypotheses that it was formed by fibers. For further insight, it was then necessary to image the sample by SEM. In order to get a picture of the fibers formed when the gel is at 5%w/v, the sample was lyophilized in to remove water without changing the structure.

It can be confirmed in Figure 11 that the hydro gel appears to be formed of fibers formed by self-assembly of Astrophloxine Acrylate.

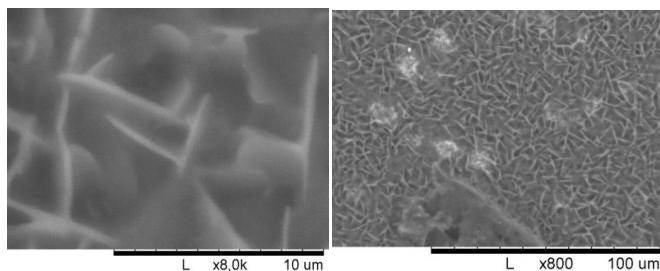


Figure 12- SEM images of the 5%w/v Astrophloxine Acrylate hydrogel fibers after lyophilisation.

#### B. QR-SY ionically self-assembled Nanofibers

The obtained QR-SY fibers were observed under an optical microscope using a polarizer. According to the optical image in **Erreur ! Source du renvoi introuvable.**, it is possible to see easily the fibers, which are birefringent.

An X-Ray Diffraction pattern was collected in order to confirm the presence of a crystalline structure. (See Figure 14) The XRD diffractogram obtained show peaks corresponding to a crystalline structure. The fibers are organized as an organic self-assembled crystal. Further analysis is needed to resolve the crystallographic structure of the fibers.

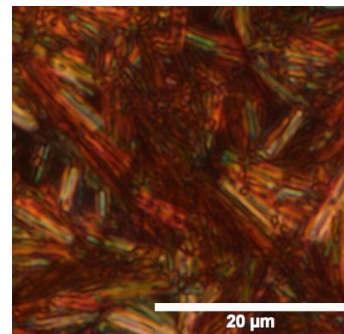


Figure 13- Optical image of the fibers using a polarizer filter.

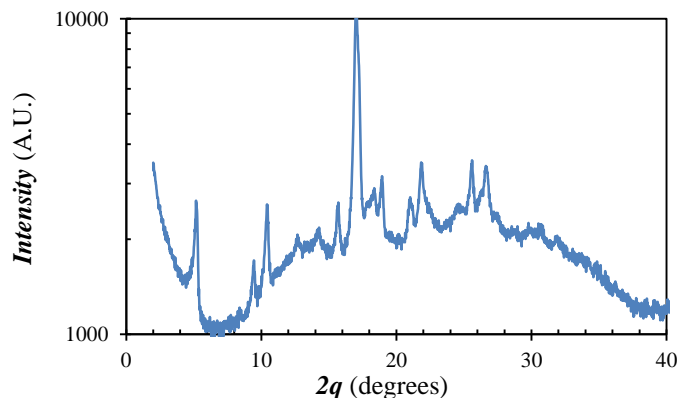


Figure 14- X-Ray diffraction.

#### - Comparison of the fibers morphology in function of the two experiments

In the SEM image (Figure 15) corresponding to the method 1 (see experimental section), fibers in the order of 10µm in length were obtained. The resolution of the SEM instrument used does not allow measuring the thickness of the fibers.

TEM with higher resolution was then used to get a better insight on fiber morphology (Figure 15). The width of the fibers is in the order of 400nm. As the zoomed image shows, the morphology of the fibers seems to be composed of stacked layers. However it was difficult to extract a diffraction pattern from the images due to the low electron density contrast

The fibers prepared by Method 2 (see experimental section) are smaller than those from Method 1 as shown in Figure 15. As the images also demonstrate, the thickness of a single fiber is down to ca.100nm which is four times smaller than the fibers from Method 1. However the length seems to be longer as they are in the range of 10µm. As for the Method 1, the diffraction pattern from TEM imaging is not well resolved which is again attributed to low contrast.

The SEM and TEM experiment confirmed that the second protocol (Method 2) developed leads to the synthesis of smaller fibers that are more in the Nanometer range. The question was then to determine if having smaller fibers allows a higher percentage of ketoprofen encapsulation.

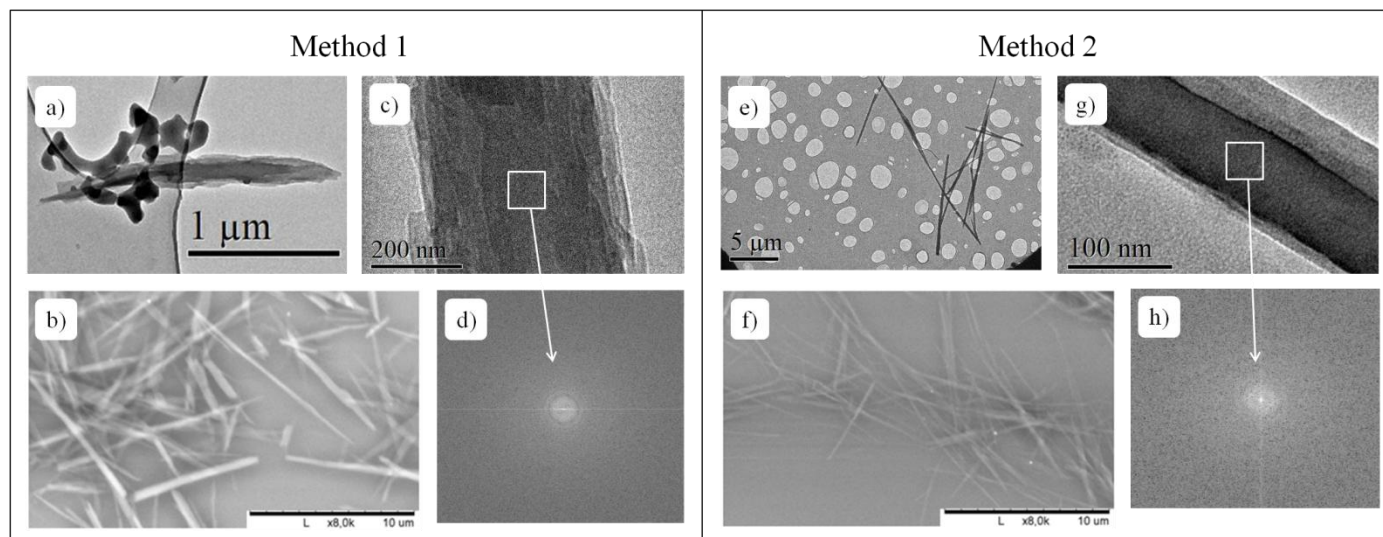


**Figure 15-** SEM and TEM images of the first and the second protocol. the images a), b), e) and f) are TEM images. Images c) and g) are SEM images. Image d) the diffraction pattern coming from picture b). Image h) is the diffraction pattern of coming from f) image.

### C. Drug encapsulation

A calibration curve was prepared to determine the amount of encapsulated KTP by HPLC (Figure 16). All the samples were prepared by dilution of an initial solution of ketoprofen at 500 μg/mL in PBS.

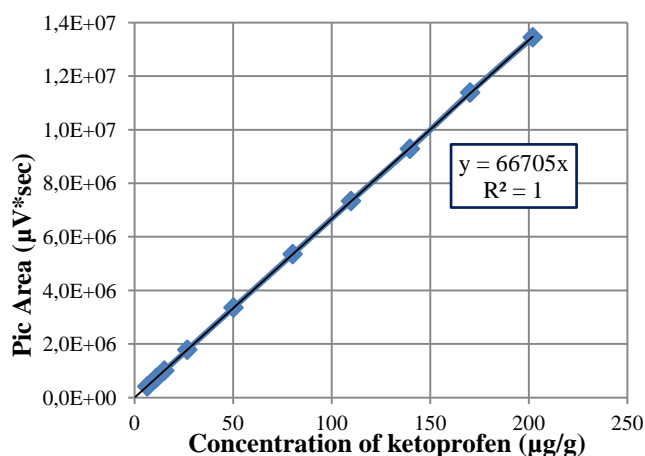


**Figure 16-** Calibration curve of the Ketoprofen in PBS.

#### a) Encapsulation in the fibers of the system 2

In both Methods, the encapsulation was done at the same time that the syntheses of the fibers. A small volume of supernatant was taken after the first centrifugation and was analyzed by HPLC. By measuring the concentration of KTP in the supernatant, it was then possible to extrapolate the quantity of drug that was encapsulated inside the fibers. The calibration curve was used in order to correlate the area of the peaks obtained by HPLC as a function of the concentration of KTP.

A concentration of 7.6mg/mL was obtained for the drug encapsulation of the Method 1. As the initial encapsulated amount of KTP was 10mg, only 24% of the drug was encapsulated inside the fibers. For the Method 2, the concentration of KTP measured in the supernatant solution was 5.4mg/mL which means that 46% of the drug was encapsulated inside the fibers.

The percentage of drug encapsulation is significantly different between the first and the second method, with a value almost twice higher for the synthesis Method 2.

Furthermore, the yield of the synthesis of the fibers in both cases was only of around 50%; considering that the encapsulation of the total amount of drug was 46% for the second method, thus, if the yield of synthesis of the fibers was 100%, the total drug encapsulation could be up to 92%.

## IV. CONCLUSION

During this project, the synthesis of the 2 different fibers formed by self-assembly of  $\pi$ - $\pi$  stacking and ISA were performed, each one with different morphological, optical, calorimetric and encapsulation properties.

For the hydrogel fibers system we could demonstrate the behaving of the gel in function of the temperature, its fluorescent properties and the viscoelastic properties. The correlation between self-assembly and fluorescence was demonstrated thanks to the study of the fluorescence in function of the temperature. The SEM demonstrated also that the system was formed of fibers with a high hydration. This systems shows birefringence properties from a ordered material, without being a liquid crystal.

Regarding the second system, the synthesis with Method 2 showed thinner fibers, leadings to higher surface to volume ratio and higher drug encapsulation. As seen, the encapsulation process was more efficient in Method 2, with an encapsulation potential higher than 90%, with the condition of

increasing the yield of the synthesis of the nanofibers formed by ISA. The synthesis protocol of the fibers still has to be improved in order to increase the yield and satisfy this 90% encapsulation. Since future applications in medicine could be possible, a drug release experiment should be the next step in the development of these systems.

#### ACKNOWLEDGMENT

Credits are first given to Carlos Rodriguez-Abreu. the author thanks the Institute for Advanced Chemistry of Catalonia, Spanish National Research Council (IQAC-CSIC) and to the master programme of Nanoscience and Nanotechnology from the University of Barcelona (UB).

#### REFERENCES

- [1] P. Boisseau and B. Loubaton, "Nanomedicine, nanotechnology in medicine," *Comptes Rendus Phys.*, vol. 12, no. 7, pp. 620–636, Sep. 2011.
- [2] C. F. J. Faul, "Ionic Self-Assembly for Functional Hierarchical Nanostructured Materials," *Acc. Chem. Res.*, vol. 47, no. 12, pp. 3428–3438, Dec. 2014.
- [3] C. F. J. Faul and M. Antonietti, "Ionic Self-Assembly: Facile Synthesis of Supramolecular Materials," *Adv. Mater.*, vol. 15, no. 9, pp. 673–683, May 2003.
- [4] J. Shen, S. Yuan, and X. Xin, "Supramolecular Materials Based on Ionic Self-Assembly: Structure, Property, and Application," in *Molecular Self-assembly in Nanoscience and Nanotechnology*, InTech, 2017.
- [5] Ying Guan, and Markus Antonietti, and C. F. Faul\*, "Ionic Self-Assembly of Dye–Surfactant Complexes: Influence of Tail Lengths and Dye Architecture on the Phase Morphology," 2002.
- [6] Y. Guan, S.-H. Yu, M. Antonietti, C. Böttcher, and C. F. J. Faul, "Synthesis of Supramolecular Polymers by Ionic Self-Assembly of Oppositely Charged Dyes," *Chem. - A Eur. J.*, vol. 11, no. 4, pp. 1305–1311, Feb. 2005.
- [7] H.-W. An and M.-D. Wang, "The Self-assembly of Cyanine Dyes for Biomedical Application In Vivo," Springer, Singapore, 2018, pp. 31–55.
- [8] I. E. Shohin *et al.*, "Biowaiver Monographs for Immediate-Release Solid Oral Dosage Forms: Ketoprofen," *J. Pharm. Sci.*, vol. 101, no. 10, pp. 3593–3603, Oct. 2012.
- [9] R. Rachmaniar, D. Tristiyanti, S. Hamdani, and Afifah, "Solubility and dissolution improvement of ketoprofen by emulsification ionic gelation," in *AIP Conference Proceedings*, 2018, vol. 1927, no. 1, p. 030024.
- [10] DrugBank, "Ketoprofen," 2005. [Online]. Available: <https://www.drugbank.ca/drugs/DB01009>. [Accessed: 02-Jul-2019].
- [11] LibreTexts Chemistry, "Fluorescence and Phosphorescence - Chemistry LibreTexts," 2019. [Online]. Available: [https://chem.libretexts.org/Bookshelves/Physical\\_and\\_Theoretical\\_Chemistry\\_Textbook\\_Maps/Supplemental\\_Modules\\_\(Physical\\_and\\_Theoretical\\_Chemistry\)/Spectroscopy/Electronic\\_Spectroscopy/Fluorescence\\_and\\_Phosphorescence](https://chem.libretexts.org/Bookshelves/Physical_and_Theoretical_Chemistry_Textbook_Maps/Supplemental_Modules_(Physical_and_Theoretical_Chemistry)/Spectroscopy/Electronic_Spectroscopy/Fluorescence_and_Phosphorescence). [Accessed: 01-Jul-2019].
- [12] Nikon, "Principles of Birefringence | MicroscopyU." [Online]. Available: <https://www.microscopyu.com/techniques/polarized-light/principles-of-birefringence>. [Accessed: 02-Jul-2019].
- [13] H. A. Barnes, J. F. (John F. Hutton, and K. Walters, *An introduction to rheology*. Elsevier, 1989.
- [14] Bohlin Instruments, "A basic introduction to Rheology," 2008.
- [15] RheoSense, "Viscosity of Newtonian and Non-Newtonian Fluids," 2019. [Online]. Available: <https://www.rheosense.com/applications/viscosity/newtonian-non-newtonian>. [Accessed: 02-Jul-2019].
- [16] Anton Paar GmbH, "Basics of rheology," 2006. [Online]. Available: <https://wiki.anton-paar.com/en/basics-of-rheology/>. [Accessed: 02-Jul-2019].
- [17] J. Miras, S. Vílchez, C. Solans, T. Tadros, and J. Esquena, "Kinetics of chitosan hydrogel formation in high internal phase oil-in-water emulsions (HIPEs) using viscoelastic measurements," *Soft Matter*, vol. 9, no. 36, p. 8678, Aug. 2013.
- [18] T. . Mezger, *Applied Rheology*, 4th ed. Anton Paar GmbH, 2017.
- [19] TA instruments, "Understanding Rheology of Structured Fluids."